Acta Cryst. (1997). B53, 596–603

Phase Transition in $K_3Na(MoO_4)_2$ and Determination of the Twinned Structures of $K_3Na(MoO_4)_2$ and $K_{2.5}Na_{1.5}(MoO_4)_2$ at Room Temperature

J. FÁBRY,[a]* V. PETŘÍČEK,[a] P. VANĚK[b] AND I. CÍSAŘOVÁ[b]

[a]*Institute of Physics of the Czech Academy of Sciences, Cukrovarnická 10, 162 00 Praha 6, Czech Republic,* [b]*Institute of Physics of the Czech Academy of Sciences, Na Slovance 2, 180 40 Praha 8, Czech Republic, and* [c]*Faculty of Science, Hlavova 2030, Praha 2, Czech Republic. E-mail: fabry@fzu.cz*

(*Received 26 June 1996; accepted 3 February 1997*)

Abstract

The room-temperature phases of sodium potassium molybdates $K_3Na(MoO_4)_2$ and $K_{2.5}Na_{1.5}(MoO_4)_2$ are isostructural with the monoclinic low-temperature phases of $K_3Na(SeO_4)_2$ and $K_3Na(CrO_4)_2$, which are twinned distorted glaserite structures. In the molybdates there are two crystallographically independent potassiums and their environment slightly differs from those in $K_3Na(SeO_4)_2$ and $K_3Na(CrO_4)_2$. The excessive Na in $K_{2.5}Na_{1.5}(MoO_4)_2$ occupies the position of the more firmly bound potassium. A reversible phase transition at 513 K was discovered in $K_3Na(MoO_4)_2$ by DSC (differential scanning calorimetry), but no such transition in $K_{2.5}Na_{1.5}(MoO_4)_2$ was detected. Both samples used in the diffractometer experiment were found to be composed of six domains being related by twinning operations of the point group 6. The twinning may be considered as a combination of a merohedral and a pseudo-merohedral twinning with two- and threefold rotations as twinning operations, respectively. However, a reversible domain switching, which is observable in the related ferroelastic crystals of $K_3Na(SeO_4)_2$ and $K_3Na(CrO_4)_2$, was not observed either in $K_3Na(MoO_4)_2$ or in $K_{2.5}Na_{1.5}(MoO_4)_2$, either due to semitransparency of the samples or high ferroelastic distortion. This distortion is manifested by the values of the atomic displacement vectors which are about twice as large as those in the selenate or the chromate.

1. Introduction

The previous structural studies of $K_3Na(CrO_4)_2$ (Fábry, Breczewski & Madariaga, 1994; Madariaga & Breczewski, 1990) and $K_3Na(SeO_4)_2$ (Fábry, Breczewski & Petříček, 1993) revealed that their high-temperature phase is trigonal, belonging to the glaserite family ($P\bar{3}m1$), while the low-temperature phase is monoclinic and ferroelastic ($C2/c$). Concomitantly with the ferroelastic phase transition into the monoclinic phase a threefold axis is lost, the c axis doubles its length and each of the mirror planes (related to each respective domain) is transformed into the glide plane c. A triple-twinned domain pattern develops.

However, the metric of the lattice preserves its hexagonality within experimental error (there was no indication of the separation of reflections) at the low-temperature phase. Therefore, the structure of the low-temperature phase can be described in the primitive hexagonal cell in one of the non-standard monoclinic space groups (Table 1). [One of these non-standard space groups can be described in Halls notation as $P2_c''$ (Hall, 1981).] The unit cell related to the standard choice of the space group ($C2/c$) is an orthohexagonal cell.

The transitions from the high-temperature phase into the low-temperature phase are rather complicated in these compounds. In $K_3Na(SeO_4)_2$ there are two phase transitions at 346 and 334 K (Krajewski, Piskunowicz & Mroz, 1993). The former phase transition is manifested by anomalies in DTA curves, thermal expansion and dielectric parameters. Already between 334 and 346 K the c axis is doubled with respect to the high-temperature phase and the reflections, now with $l = 2n + 1$, develop. These reflections are much less intensive above 334 K than below this temperature (Fábry, Breczewski & Petříček, 1993). The phase transition at 334 K was deduced from the temperature dependence of the elastic constants (Mroz, Kiefte, Clouter & Tuszynski, 1992).

In $K_3Na(CrO_4)_2$ a weakly first-order ferroelastic continuous phase transition takes place (Mroz, Kiefte, Clouter & Tuszynski, 1992). This phase transition begins, when cooling, at 239 K and continues down to $\sim$ 210 K (Krajewski, Mroz, Piskunowicz & Breczewski, 1990) until the ferroelastic distortion becomes saturated. During this continuous phase transition the tetrahedral anions gradually tilt and displace from the sites occupied in the high-temperature phase. Similarly, both potassiums are gradually shifted from their positions in the high-temperature phase.

From the structure determinations of $K_3Na(CrO_4)_2$ (Fábry, Breczewski & Madariaga, 1994; Madariaga & Breczewski, 1990), $K_3Na(SeO_4)_2$ (Fábry, Breczewski & Petříček, 1993) as well as $K_3Na(SO_4)_2$ (Okada & Ossaka, 1980) it was deduced that this phase transition from the trigonal to the monoclinic phase is related predominantly to the bonding of the most weakly bound

Table 1. *Relevant transformations and relations used in the structure determination of the room-temperature phase of $K_3Na(MoO_4)_2$*

(i) Expression for transformation of indices from the primitive pseudohexagonal unit cell (*h* superscript) to the standard monoclinic *C*-centred (pseudo-orthorhombic) unit cell (*o* superscript)

$$[hkl]^0 = [hkl]^h \begin{bmatrix} -1 & -1 & 0 \\ 1 & -1 & 0 \\ 0 & 0 & 1 \end{bmatrix}.$$

(ii) Relations for superposition of indices related to the standard monoclinic *C*-cell from pertinent domains. The index numbers *n* (n = 1–5) are referred to the domains which are related to the basic domain by $n \times 60°$ in an anticlockwise direction

$$[hkl]^1 = [hkl] \begin{bmatrix} \frac{1}{2} & -\frac{1}{2} & 0 \\ \frac{3}{2} & \frac{1}{2} & 0 \\ 0 & 0 & 1 \end{bmatrix} \qquad [hkl]^2 = [hkl] \begin{bmatrix} -\frac{1}{2} & -\frac{1}{2} & 0 \\ \frac{3}{2} & -\frac{1}{2} & 0 \\ 0 & 0 & 1 \end{bmatrix}$$

$$[hkl]^3 = [hkl] \begin{bmatrix} -1 & 0 & 0 \\ 0 & -1 & 0 \\ 0 & 0 & 1 \end{bmatrix} \qquad [hkl]^4 = [hkl] \begin{bmatrix} -\frac{1}{2} & \frac{1}{2} & 0 \\ -\frac{3}{2} & -\frac{1}{2} & 0 \\ 0 & 0 & 1 \end{bmatrix}$$

$$[hkl]^5 = [hkl] \begin{bmatrix} \frac{1}{2} & \frac{1}{2} & 0 \\ -\frac{3}{2} & \frac{1}{2} & 0 \\ 0 & 0 & 1 \end{bmatrix}.$$

(iii) Expression for ferroelastic transformations of coordinates in the pseudohexagonal unit cell (labels '*A*' and '*B*' are related to the domains rotated by 120 and 240° in an anticlockwise direction)

$$\begin{bmatrix} x \\ y \\ z \end{bmatrix}^A = \begin{bmatrix} 0 & -1 & 0 \\ 1 & -1 & 0 \\ 0 & 0 & 1 \end{bmatrix} \begin{bmatrix} x \\ y \\ z \end{bmatrix} \qquad \begin{bmatrix} x \\ y \\ z \end{bmatrix}^B = \begin{bmatrix} -1 & 1 & 0 \\ -1 & 0 & 0 \\ 0 & 0 & 1 \end{bmatrix} \begin{bmatrix} x \\ y \\ z \end{bmatrix}.$$

(iv) Twofold axis operators of the non-standard space group $\tilde{P}2_c''$ and the other two space groups, the symmetry operators of which are rotated by 120 and 240° in an anticlockwise direction, with respect to those in $\tilde{P}2_c''$. The remaining group operators are obtained by multiplication of these operators with inversion and identity operators. These non-standard space groups are isomorphous with the $C2/c$ space group

$$\tilde{P}2_c'' \qquad \begin{bmatrix} 0 & 1 & 0 \\ 1 & 0 & 0 \\ 0 & 0 & -1 \end{bmatrix} \begin{bmatrix} 0 \\ 0 \\ 1/2 \end{bmatrix}$$

$$\tilde{P}2_c'' \ (+120°) \qquad \begin{bmatrix} 1 & -1 & 0 \\ 0 & -1 & 0 \\ 0 & 0 & -1 \end{bmatrix} \begin{bmatrix} 0 \\ 0 \\ 1/2 \end{bmatrix}$$

$$\tilde{P}2_c'' \ (+240°) \qquad \begin{bmatrix} -1 & 0 & 0 \\ -1 & 1 & 0 \\ 0 & 0 & -1 \end{bmatrix} \begin{bmatrix} 0 \\ 0 \\ 1/2 \end{bmatrix}.$$

(v) Transformation of coordinates from the *C*-centred (pseudo-orthohexagonal) unit cell (labelled as 'O') to different choices of the pseudo-hexagonal unit cells (labels '*A*' and '*B*' are related to the domains rotated by 120 and 240° in an anticlockwise direction)

$$\tilde{P}2_c'' \qquad \begin{bmatrix} x \\ y \\ z \end{bmatrix} = \begin{bmatrix} -1 & -1 & 0 \\ 1 & -1 & 0 \\ 0 & 0 & 1 \end{bmatrix} \begin{bmatrix} x \\ y \\ z \end{bmatrix}^o$$

$$\tilde{P}2_c'' \ (+120°) \qquad \begin{bmatrix} x \\ y \\ z \end{bmatrix}^A = \begin{bmatrix} -1 & -1 & 0 \\ -2 & 0 & 0 \\ 0 & 0 & 1 \end{bmatrix} \begin{bmatrix} x \\ y \\ z \end{bmatrix}^o$$

$$\tilde{P}2_c'' \ (+240°) \qquad \begin{bmatrix} x \\ y \\ z \end{bmatrix}^B = \begin{bmatrix} 0 & -2 & 0 \\ -1 & -1 & 0 \\ 0 & 0 & 1 \end{bmatrix} \begin{bmatrix} x \\ y \\ z \end{bmatrix}^o.$$

cation in the structure, K(2). This cation is coordinated by 6 + 6 oxygens. Such a high coordination number causes a rather loose bonding of the cation which is placed in a large cavity. The larger the tetrahedral anion, the larger the cavity and, therefore, the temperatures of the phase transitions from the monoclinic to the trigonal phases should increase with the growing size of the anions ($SO_4^{2-} < CrO_4^{2-} < SeO_4^{2-} < MoO_4^{2-} \simeq WO_4^{2-}$). [In $K_3Na(SO_4)_2$ no phase transition was detected down to 100 K (Krajewski (1990).] Thus, with regard to the phase transition temperature of $K_3Na(SeO_4)_2$ it was suggested (Fábry, Breczewski & Madariaga, 1994) that $K_3Na(MoO_4)_2$ and $K_3Na(WO_4)_2$ should also be monoclinic at room temperature, *i.e.* the distorted glaserite structures.

It follows from the previous paragraphs that the reflections hkl, $l = 2n + 1$, indicate the monoclinic nature of these phases. However, the references regarding $K_3Na(MoO_4)_2$ (Mehrotra, Eysel & Hahn, 1977; PDF 28-801) and $K_3Na(WO_4)_2$ (Mehrotra, Eysel & Hahn, 1977; PDF 28-802) gave parameter *c* not doubled and both structures were considered as trigonal. (The numbers which follow the 'PDF' refer to the respective powder diffraction file.)

Related compounds with excessive Na have been described: $KNaCrO_4$ (trigonal, PDF 26-1468), $(K_{0.25}Na_{0.75})_2CrO_4$ (monoclinic, PDF 26-1467), $(K_{0.20}Na_{0.80})_2CrO_4$ (monoclinic, PDF 26-1332), $KNaSO_4$ (Okada & Ossaka, 1980). In the latter compound described in $P3m1$ the excessive sodium subtitutes one of two K(1) sites and the structure is ordered.

The aim of this study was to test the hypothesis on the monoclinic nature of $K_3Na(MoO_4)_2$ and to determine the temperature at which the supposed phase transition takes place. In addition, the structure of a non-stoichiometric compound $K_{2.5}Na_{1.5}(MoO_4)_2$ was determined in order to find out which of the potassium sites would be preferentially occupied by the excessive sodium.

2. Experimental

Mixtures of stoichiometric amounts of K_2MoO_4 and $Na_2MoO_4.2H_2O$ were heated in a platinum crucible up to 1223 K. The samples were held at this temperature for 1 h and then cooled down to room temperature at 10 and 5 K h^{-1} for $K_3Na(MoO_4)_2$ and $K_{2.5}Na_{1.5}(MoO_4)_2$, respectively. The products contained single crystals of size 0.1–1 mm and the single crystals used in the X-ray experiments were taken from them. In addition, another batch of $K_3Na(MoO_4)_2$ cooled down at 5 K h^{-1} was prepared. The latter sample was used in the DSC experiment.

The DSC measurements were carried out on a Perkin–Elmer DSC 7 differential scanning calorimeter. Powdered samples (~ 40 mg typically) were sealed in Al pans and measured between 298 and 793 K both on

heating and cooling at the scanning rate 10 K min^{-1}. The calorimeter was calibrated using the extrapolated onsets of melting of indium and tin at a scanning rate of 10 K min^{-1} and the melting enthalpy of indium.

Weissenberg and precession photographs revealed the existence of $l = 2n + 1$ reflections, which were much less intensive than those with l even. The $00l$ reflections, $l = 2n + 1$, were systematically absent. The information regarding crystal data, intensity collection and refinements of both compounds is summarized in Table 2.

The Patterson syntheses of both samples yielded maxima which could be unequivocally assigned to the Mo—O bonds. These maxima conformed well to the group $6/m\ m\ m$. As has already been pointed out in the *Introduction*, the $l = 2n + 1$ reflections indicate a pseudo-merohedral triple twinning; such a twinning, being a residue of the disappeared trigonal axis, would cause the maxima on the Patterson map to correspond well to the $\bar{3}m1$ group. Therefore, it was assumed that an additional merohedral twofold twinning was present. The axis of the latter twinning coincided with the direction of the disappeared threefold axis. This implies that the observed twinning is a superposition of merohedral twinning (the twinning operation is a twofold rotation) and pseudo-merohedral twinning (the twinning operation is a threefold rotation). Therefore, it was assumed that both samples were composed of six domains. [Such a twinning was also observed in $K_3Na(CrO_4)_2$ (Fábry, Breczewski & Madariaga, 1994).]

A hypothetical structure based on the high-temperature phase of $K_3Na(SeO4)_2$ (Fábry, Breczewski & Petříček, 1993) was constructed. At the beginning of the refinement of each compound the anion was restricted to the rigid-body refinement, while the domain fractions as well as the positions of the cations were refined. After the refinement had converged all the atoms were refined individually.

The transformations used in the calculations are given in Table 1.

$\Delta F(\mathbf{h}) = (|F_o(\mathbf{h})| - |F_c(\mathbf{h})|)\exp(i\varphi(\mathbf{h}))$ used in the difference Fourier synthesis

$$\Delta\rho = \sum_h \Delta F(\mathbf{h})\exp(-2\pi i\mathbf{hr})$$

was modified as $[(|F_o(\mathbf{h})| - |F_c(\mathbf{h})|)/|F_c(\mathbf{h})|]|F_c^1(\mathbf{h})\exp(i\varphi^1(\mathbf{h}))$, where $|F_o(\mathbf{h})|$ and $|F_c(\mathbf{h})|$ are the scaled observed and calculated square roots of the reduced observed and calculated intensities, $|F_c^1(\mathbf{h})|$ is the calculated absolute value of the first domain structure factor, and $\varphi(\mathbf{h})$ and $\varphi^1(\mathbf{h})$ are the respective phase angles.

In all the calculations the stoichiometry of the title crystals was supposed to be equal to the proportion of the compounds used in the syntheses.

The calculations were performed mostly by the *SDS* program package (Petříček, 1995). The corrections of the bond distances for the thermal movement of the $[MoO_4]^{2-}$ were calculated by the program *PARST*95 (Nardelli, 1995). The data reduction was performed by the program *ZPRAC* (Fábry, 1993). The figures were drawn by *PICTUR* (Dušek, 1993) and *ORTEP*III (Burnett & Johnson, 1996). In addition, the Inorganic Crystal Structure Database (*CRYSTIN*, 1995; Bergerhoff, Hundt, Sievers & Brown, 1983) as well as The Powder Diffraction File (1996) were used. Data collection and unit-cell refinement were performed using Enraf–Nonius (1989) software.

3. Discussion

The DSC curves exhibited a reproducible and reversible lambda-type anomaly in $K_3Na(MoO_4)_2$ at 513 K (ΔC_p = 28 J mol^{-1} K^{-1}), which indicates the structural phase transition. No DSC anomaly was detected in $K_{2.5}Na_{1.5}(MoO_4)_2$.

By analogy with $K_3Na(CrO_4)_2$ and $K_3Na(SeO_4)_2$, it is assumed that $K_3Na(MoO_4)_2$ above 513 K belongs to the glaserite structure ($P\bar{3}m1$).

The structure of $K_3Na(MoO_4)_2$ is depicted in Figs. 1 and 2 (the non-stoichiometric compound is not depicted here because of the similarity with the stoichiometric compound). The structural parameters are given in Tables 3 and 4 for $K_3Na(MoO_4)_2$ and $K_{2.5}Na_{1.5}(MoO_4)_2$, respectively.

Several models were refined in order to determine the distribution of Na among the cation sites in $K_{2.5}Na_{1.5}(MoO_4)_2$. All the models coincided in finding that it is the K(1) site which is occupied by the excessive sodium. [The K(1) is the more firmly bound potassium in the structure (*e.g.* Fábry, Breczewski & Petříček, 1993).]

The model which assumes that no potassium can enter into the Na site and that sodiums as well as potassiums in the same sites have the same temperature parameters was chosen as the most satisfactory (Table 4), since it yielded no negative occupational parameters; the constraint conditions are given in Table 2.* The model where the Na site was allowed to be occupied by potassium, while complying with the supposed stoichiometry, yielded a negative value of the occupational parameter of K [–0.14 (5)], which was balanced by the occupation of Na (1.14) at site 0,0,0. The ratio of K(1)/Na(1) resulted in 0.82 (2)/0.18 (2), *cf.* Table 4. The other model where the cation sites were supposed to be fully occupied and the distributions of sodiums and potassiums were refined independently (both cations in each site had the same atomic displacement factors) also indicated that excess Na enters the position of K(1); the refined ratio K(1)/Na(1) resulted in 0.86 (2)/0.14 (2). The occupational parameter of K at site 0,0,0 resulted in

* Lists of anisotropic displacement parameters and structure factors have been deposited with the IUCr (Reference: SH0083). Copies may be obtained through The Managing Editor, International Union of Crystallography, 5 Abbey Square, Chester CH1 2HU, England.

Table 2. *Experimental details*

	$K_3Na(MoO_4)_2$	$K_{2.5}Na_{1.5}(MoO_4)_2$
Crystal data		
Chemical formula	$K_3Na(MoO_4)_2$	$K_{2.5}Na_{1.5}(MoO_4)_2$
Chemical formula weight	458.156	450.102
Cell setting	Monoclinic	Monoclinic
Space group	$C2/c$	$C2/c$
a (Å)	10.4455 (14)	10.3849 (13)
b (Å)	6.0307 (8)	5.9957 (7)
c (Å)	15.240 (4)	15.043 (2)
β (°)	90.00 (2)	90.00 (2)
V (Å^3)	960.02	936.65
Z	4	4
D_x (Mg m^{-3})	3.169	3.191
Radiation type	Mo $K\alpha$	Mo $K\alpha$
Wavelength (Å)	0.71073	0.71073
No. of reflections for cell parameters	25	25
θ range (°)	14–16	14–16
μ (mm^{-1})	3.969	3.869
Temperature (K)	290 (2)	290 (2)
Crystal form	Plate	Plate
Crystal size (mm)	0.30 × 0.24 × 0.11	0.35 × 0.35 × 0.15
Crystal colour	Colourless	Colourless
Data collection		
Diffractometer	Enraf–Nonius CAD-4 MACHIII-PC	Enraf–Nonius CAD-4 MACHIII-PC
ω-scan width (°)	1.10 + 0.35tanθ	1.10 + 0.35tanθ
Horizontal aperture (mm)	2.00 + 1.00tanθ	2.00 + 1.00tanθ
Vertical aperture (mm)	4	4
Minimal/maximal scan speed (° min^{-1})	0.824, 5.493	0.749, 5.493
Data collection method	ω–2θ scans	ω–2θ scans
Absorption correction	Analytical from crystal shape (Templeton & Templeton, 1978)	Analytical from crystal shape (Templeton & Templeton, 1978)
T_{min}	0.667	0.517
T_{max}	0.811	0.747
Maximal final scan time (s)	90	90
No. of measured reflections	4041	1837
No. of independent reflections	2076	1836
No. of observed reflections	2056	1824
Criterion for observed reflections	$F > 3\sigma(F)$	$F > 3\sigma(F)$
R_{int}	0.0061	–
$R_{e.s.d.}$ *	0.060	–
θ_{max} (°)	27	26
Range of h, k, l	$-12 \rightarrow h \rightarrow 12$ $-7 \rightarrow k \rightarrow 7$ $-19 \rightarrow l \rightarrow 18$	$-12 \rightarrow h \rightarrow 12$ $-7 \rightarrow k \rightarrow 7$ $0 \rightarrow l \rightarrow 18$
Constraint number	1	22
(f_i is a domain fraction)	$f_1 = 1 - \sum_{i=2}^{6} f_i$	$f_1 = 1 - \sum_{i=2}^{6} f_i$ †
No. of standard reflections	3	3
Frequency of standard reflections (min)	3600	3600
Intensity decay (%)	4	2
Refinement		
Refinement on	F	F
R	0.0291	0.0442
wR	0.0362	0.0611
S	1.16	1.96
No. of reflections used in refinement	2076	1836
No. of parameters used	72	73
Weighting scheme	$w = 1/[\sigma^2(F_o) + 0.0009(F_o)^2]$	$w = 1/[\sigma^2(F_o) + 0.0009(F_o)^2]$
$(\Delta/\sigma)_{max}$	0.01	0.01
$\Delta\rho_{max}$ (e Å^{-3})	2.76	2.41
$\Delta\rho_{min}$ (e Å^{-3})	−1.10	−1.31
Extinction method	Becker & Coppens (1974), Lorentzian isotropic	Becker & Coppens (1974), Lorentzian isotropic
Extinction coefficient	0.40 (9) × 10^{-5}	1.2 (2) × 10^{-5}
Domain factors		
f_1	0.4087 (9)	0.064 (2)
f_2	0.1214 (8)	0.350 (2)
f_3	0.1103 (9)	0.059 (1)
f_4	0.0672 (8)	0.169 (2)
f_5	0.1080 (9)	0.117 (1)
f_6	0.1844 (8)	0.241 (2)
Source of atomic scattering factors	*International Tables for X-ray Crystallography* (1974, Vol. IV, Tables 2.2A and 2.3.1)	*International Tables for X-ray Crystallography* (1974, Vol. IV, Tables 2.2A and 2.3.1)

* $R_{e.s.d.}$ is defined as $\sum_h$ e.s.d. $(F_h)/\sum_h|F_h|$. † Occupancy factor (o.f.) = o.f.[Na(2)] = 1.00 − o.f.[K(2)]; o.f.[Na(1)] = 0.50 − o.f.[Na(2)]; o.f.[K(1)] = 1.00 − o.f.[Na(1)]. Temperature factors of Na and K at the same site are equal (the respective coordinate parameters are constrained).

–0.06 (4) and Na(2) at the site of K(2) equaled –0.05 (4). Neither of these models of different cation distribution, however, differed significantly in the resulting positional parameters. The corresponding *R*-factor values of these refinements differed in the fourth figure. The results of these refinements are included in the deposited material.

This result corresponds with the observation that excess Na in $KNaSO_4$ (Okada & Ossaka, 1980) enters into one of two K(1) sites, but not into the K(2) site.

In order to assess the influence of non-uniformity of a domain distribution, as well as errors in the absorption correction, on the refined parameters the symmetry-independent reflection sets were chosen for the structure refinement of $K_3Na(MoO_4)_2$ and $K_{2.5}Na_{1.5}(MoO_4)_2$. Ideally all the structural parameters calculated from any independent set would converge to the same value. These calculations serve therefore as an independent indicator of the quality of the structure determination. The results are summarized in Table 5. The positional parameters differed by less than double the mean of their e.s.d.'s. The refinements given in Table 5 showed no important influence of the selection of independent reflections on the domain-fraction parameters in the stoichiometric compound, in contrast with the non-stoichiometric compound. Thus, the structure determination of $K_3Na(MoO_4)_2$ seems to be less biased than that of $K_{2.5}Na_{1.5}(MoO_4)_2$. The occupational parameters

Table 3. *Fractional atomic coordinates and equivalent isotropic displacement parameters (Å²) for* $K_3Na(MoO_4)_2$

$U_{eq} = (1/3)\Sigma_i\Sigma_j U^{ij} a_i^* a_j^* \mathbf{a}_i.\mathbf{a}_j.$

	x	*y*	*z*	U_{eq}
K(1)	0.1711 (2)	0.4778 (1)	0.41526 (7)	0.0224 (3)
K(2)	0.0 (0)	0.9474 (3)	0.25 (0)	0.0268 (5)
Na	0.0 (0)	0.0 (0)	0.0 (0)	0.0138 (9)
Mo	0.16278 (5)	0.48090 (5)	0.13946 (2)	0.0114 (1)
O(1)	0.1724 (6)	0.5498 (6)	0.2502 (2)	0.039 (1)
O(2)	0.0822 (3)	0.6954 (5)	0.0837 (2)	0.028 (1)
O(3)	0.0806 (3)	0.2317 (5)	0.1195 (2)	0.027 (1)
O(4)	0.3158 (4)	0.4606 (6)	0.0910 (3)	0.032 (1)

Table 4. *Fractional atomic coordinates and equivalent isotropic displacement parameters (Å²) for* $K_{2.5}Na_{1.5}(MoO_4)_2$

$U_{eq} = (1/3)\Sigma_i\Sigma_j U^{ij} a_i^* a_j^* \mathbf{a}_i.\mathbf{a}_j.$

	x	*y*	*z*	U_{eq}
K(1)	0.1686 (6)	0.4765 (3)	0.4137 (2)	0.0342 (8)
Na(1)	0.1686 (6)	0.4765 (3)	0.4137 (2)	0.0342 (8)
K(2)	0.0 (0)	0.9487 (5)	0.25 (0)	0.041 (1)
Na(2)	0.0 (0)	0.9487 (5)	0.25 (0)	0.041 (1)
Na	0.0 (0)	0.0 (0)	0.0 (0)	0.021 (2)
Mo	0.1660 (1)	0.4767 (1)	0.13846 (3)	0.0217 (3)
O(1)	0.176 (2)	0.538 (1)	0.2513 (5)	0.060 (4)
O(2)	0.091 (1)	0.695 (1)	0.0834 (5)	0.056 (3)
O(3)	0.0802 (9)	0.232 (1)	0.1205 (3)	0.045 (3)
O(4)	0.3200 (9)	0.447 (2)	0.0914 (8)	0.066 (3)

The refined occupational parameters in K(1)/Na(1) and K(2)/Na(2) sites are 0.76 (2)/0.24 (2) and 0.98 (2)/0.02 (2), respectively.

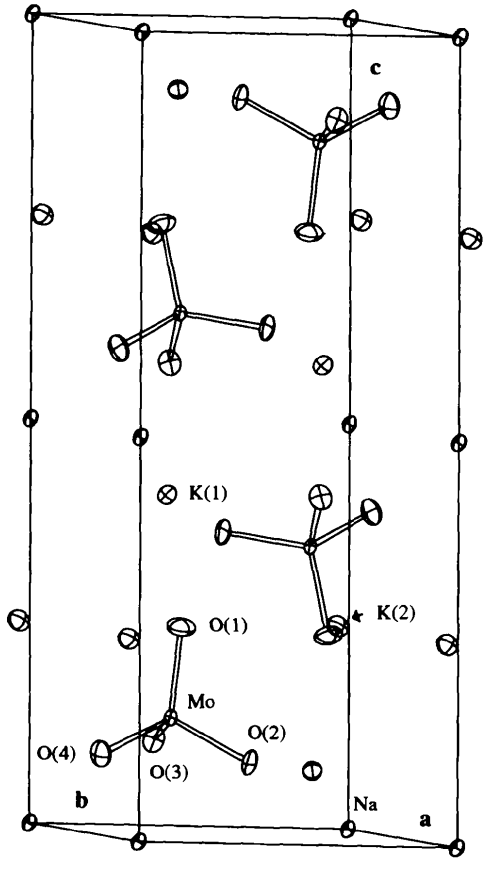

Fig. 1. View of the pseudo-hexagonal unit cell (space group $\bar{P}2_c''$) of $K_3Na(MoO_4)_2$, showing 30% probability displacement ellipsoids, drawn using *ORTEP*III (Burnett & Johnson, 1996). The atoms are related to those given in Table 3 by operations given in Table 1(v), including lattice translations if appropriate.

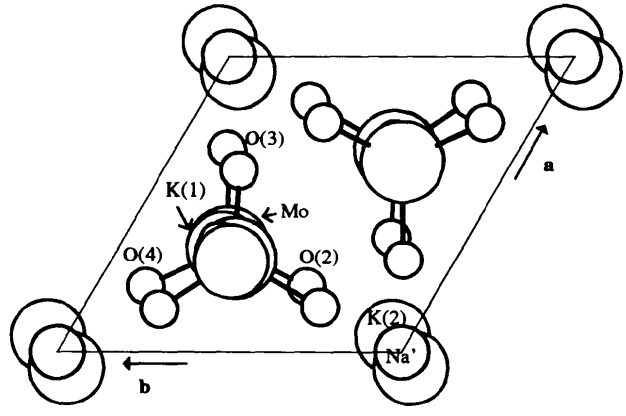

Fig. 2. View of the pseudo-hexagonal unit cell of $K_3Na(MoO_4)_2$ (space group $\bar{P}2_c''$) along the *c* axis drawn by *PICTUR* (Dušek, 1993). Na' is an equivalent atom by the translation (0,0,1) to Na given in Table 3.

Table 5. *Results of the refinements for $K_3Na(MoO_4)_2$ and $K_{2.5}Na_{1.5}(MoO_4)_2$ from the separate symmetry-independent reciprocal space regions (the weights used in the refinement are as in Table 2)*

Compound	$K_3Na(MoO_4)_2$		$K_{2.5}Na_{1.5}(MoO_4)_2$	
Region	$(h \geq 0 \cap k \geq 0) \cup (h \leq 0 \cap k \leq 0) \cup l < 0 \cup l \geq 0$	$(h \leq 0 \cap k \geq 0) \cup (h \geq 0 \cap k \leq 0) \cup l < 0 \cup l \geq 0$	$k \geq 0 \cup h < 0 \cup h \geq 0 \cup l \geq 0$	$k \leq 0 \cup 0 < h \cup h \geq 0 \cup l \geq 0$
Number of reflections (all/observed)	1192/1170	1192/1170	998/990	1017/1010
R_{int} (observed only/all)	0.0055/0.0055	0.0066/0.0066	-	-
R (observed only/all)	0.0306/0.0314	0.0256/0.0263	0.0421/0.0424	0.0413/0.0416
wR (observed only/all)	0.0465/0.0469	0.0429/0.0432	0.0586/0.0587	0.0556/0.0557
S	1.51	1.39	1.91	1.81
Domain fractions				
f_1	0.412 (2)	0.407 (2)	0.060 (3)	0.076 (3)
f_2	0.122 (2)	0.120 (2)	0.320 (3)	0.396 (3)
f_3	0.110 (2)	0.113 (2)	0.059 (2)	0.053 (2)
f_4	0.065 (1)	0.071 (1)	0.166 (2)	0.153 (2)
f_5	0.104 (2)	0.104 (2)	0.120 (2)	0.107 (2)
f_6	0.187 (2)	0.185 (2)	0.275 (3)	0.215 (3)
Extinction correction: g_{iso}	0.05 (2) $\times 10^{-4}$	0.04 (1) $\times 10^{-4}$	0.14 (3) $\times 10^{-4}$	0.10 (2) $\times 10^{-4}$
Occupancy parameters:				
K(1)/Na(1)			0.77 (1)/0.23 (1)	0.75 (1)/0.25 (1)
K(2)/Na(2)			0.96 (3)/0.04 (3)	1.00 (3)/0.00 (3)
$\Delta\rho_{max}/\Delta\rho_{min}$	2.62/−1.61	1.87/−1.28	1.42/−1.38	2.41/−2.42

Table 6. *Selected geometric parameters (Å, °)*

$K_3Na(MoO_4)_2$			
K(1)—O(1)	2.553 (4)	K(2)—O(2)	3.078 (3)
K(1)—O(1^{i})	3.961 (4)	K(2)—O(2^{ii})	3.078 (3)
K(1)—O(2^{ii})	2.954 (4)	K(2)—O(3^{v})	2.757 (3)
K(1)—O(2^{i})	3.089 (4)	K(2)—O(3^{vii})	2.757 (3)
K(1)—O(2^{iii})	2.923 (3)	K(2)—O(4^{vi})	3.095 (5)
K(1)—O(3^{ii})	3.066 (4)	K(2)—O(4^{iv})	3.095 (5)
K(1)—O(3^{iv})	3.058 (4)	Na—O(2^{viii})	2.396 (3)
K(1)—O(3^{iii})	3.695 (3)	Na—O(2^{ix})	2.396 (3)
K(1)—O(4^{i})	3.124 (4)	Na—O(3)	2.446 (3)
K(1)—O(4^{iv})	2.916 (4)	Na—O(3^{x})	2.446 (3)
K(1)—O(4^{iii})	3.098 (5)	Na—O(4^{xi})	2.384 (5)
K(2)—O(1)	2.999 (5)	Na—O(4^{xii})	2.384 (5)
K(2)—O(1^{v})	4.055 (5)	Mo—O(1)	1.741 (4)*
K(2)—O(1^{vi})	3.477 (7)	Mo—O(2)	1.762 (3)*
K(2)—O(1^{ii})	2.999 (5)	Mo—O(3)	1.757 (3)*
K(2)—O(1^{vii})	4.055 (5)	Mo—O(4)	1.765 (4)*
K(2)—O(1^{iv})	3.477 (7)		
$K_{2.5}Na_{1.5}(MoO_4)_2$			
K(1)—O(1)	2.473 (8)	K(2)—O(2)	3.081 (8)
K(1)—O(1^{i})	3.959 (11)	K(2)—O(2^{ii})	3.081 (8)
K(1)—O(2^{ii})	3.000 (11)	K(2)—O(3^{v})	2.714 (6)
K(1)—O(2^{i})	3.012 (11)	K(2)—O(3^{vii})	2.714 (6)
K(1)—O(2^{iii})	2.867 (8)	K(2)—O(4^{vi})	3.030 (11)
K(1)—O(3^{ii})	3.016 (10)	K(2)—O(4^{iv})	3.030 (11)
K(1)—O(3^{iv})	3.068 (10)	Na—O(2^{viii})	2.412 (8)
K(1)—O(3^{iii})	3.685 (6)	Na—O(2^{ix})	2.412 (8)
K(1)—O(4^{i})	3.179 (11)	Na—O(3)	2.431 (6)
K(1)—O(4^{iv})	2.823 (11)	Na—O(3^{x})	2.431 (6)
K(1)—O(4^{iii})	3.135 (11)	Na—O(4^{xi})	2.342 (10)
K(2)—O(1)	3.063 (14)	Na—O(4^{xii})	2.342 (10)
K(2)—O(1^{v})	3.980 (12)	Mo—O(1)	1.740 (8)*
K(2)—O(1^{vi})	3.410 (22)	Mo—O(2)	1.732 (8)*
K(2)—O(1^{ii})	3.063 (14)	Mo—O(3)	1.740 (7)*
K(2)—O(1^{vii})	3.980 (12)	Mo—O(4)	1.759 (10)*
K(2)—O(1^{iv})	3.410 (22)		

Symmetry codes: (i) $\frac{1}{2}-x, y-\frac{1}{2}, \frac{1}{2}-z$; (ii) $-x, y, \frac{1}{2}-z$; (iii) $x, 1-y, \frac{1}{2}+z$; (iv) $\frac{1}{2}-x, \frac{1}{2}+y, \frac{1}{2}-z$; (v) $x, 1+y, z$; (vi) $x-\frac{1}{2}, \frac{1}{2}+y, z$; (vii) $-x, 1+y, \frac{1}{2}-z$; (viii) $x, y-1, z$; (ix) $-x, 1-y, -z$; (x) $-x, -y, -z$; (xi) $x-\frac{1}{2}, y-\frac{1}{2}, z$; (xii) $\frac{1}{2}-x, \frac{1}{2}-y, -z$. * Distances corrected for thermal movement (Nardelli, 1995) are, respectively: 1.763, 1.776, 1.770, 1.781, 1.773, 1.759, 1.756, 1.800).

Table 7. *Absolute values of the atomic displacement vectors Δ (Å) in $K_3Na(MoO_4)_2$ and $K_{2.5}Na_{1.5}(MoO_4)_2$*

The labelled atoms '*A*' and '*B*' are related to the domains rotated by 120 and 240° in an anticlockwise direction, respectively (see also Table 1). Δ is a vector between the atoms linked by the lost symmetry operation (Abrahams & Keve, 1971) in this study by the threefold rotation.

$K_3Na(MoO_4)_2$	$\lvert\Delta\rvert$	$K_{2.5}Na_{1.5}(MoO_4)_2$	$\lvert\Delta\rvert$
K(1)—K(1)^{A}	0.245 (1)	K(1)/Na(1)—K(1)^{A}/Na(1)^{A}	0.246 (4)
K(1)—K(1)^{B}	0.245 (2)	K(1)/Na(1)—K(1)^{B}/Na(1)^{B}	0.246 (5)
K(1)^{A}—K(1)^{B}	0.245 (3)	K(1)^{A}/Na(1)^{A}—K(1)^{B}/Na(1)^{B}	0.246 (10)
K(2)—K(2)^{A}	0.550 (2)	K(2)/Na(2)—K(2)^{A}/Na(2)^{A}	0.533 (4)
K(2)—K(2)^{B}	0.550 (2)	K(2)/Na(2)—K(2)^{B}/Na(2)^{B}	0.533 (4)
K(2)^{A}—K(2)^{B}	0.550 (2)	K(2)^{A}/Na(2)^{A}—K(2)^{B}/Na(2)^{B}	0.533 (4)
Mo—Mo^{A}	0.2115 (6)	Mo—Mo^{A}	0.242 (1)
Mo—Mo^{B}	0.2115 (4)	Mo—Mo^{B}	0.242 (1)
Mo^{A}—Mo^{B}	0.2115 (8)	Mo^{A}—Mo^{B}	0.242 (2)
O(1)—O(1)^{A}	0.530 (7)	O(1)—O(1)^{A}	0.431 (23)
O(1)—O(1)^{B}	0.530 (6)	O(1)—O(1)^{B}	0.431 (16)
O(1)^{A}—O(1)^{B}	0.530 (11)	O(1)^{A}—O(1)^{B}	0.431 (34)
O(2)—O(4)^{A}	0.438 (6)	O(2)—O(4)^{A}	0.470 (14)
O(2)—O(3)^{B}	0.686 (4)	O(2)—O(3)^{B}	0.713 (8)
O(3)^{B}—O(4)^{A}	0.589 (6)	O(3)^{B}—O(4)^{A}	0.611 (15)
O(3)—O(2)^{A}	0.686 (4)	O(3)—O(2)^{A}	0.713 (9)
O(3)—O(4)^{B}	0.589 (5)	O(3)—O(4)^{B}	0.611 (13)
O(2)^{A}—O(4)^{B}	0.438 (7)	O(2)^{A}—O(4)^{B}	0.470 (18)
O(4)—O(3)^{A}	0.589 (6)	O(4)—O(3)^{A}	0.611 (13)
O(4)—O(2)^{B}	0.438 (5)	O(4)—O(2)^{B}	0.470 (13)
O(2)^{B}—O(3)^{A}	0.686 (5)	O(2)^{B}—O(3)^{A}	0.713 (14)

of $K_{2.5}Na_{1.5}(MoO_4)_2$ differed significantly. These differences in domain-fraction parameters may be caused by reasons which are hard to assess: non-uniform domain distribution, variation in composition of different parts of the sample and by the errors in absorption correction.

Table 8. *Cation bond valence sums (Brown & Altermatt, 1985) in $K_3Na(SO_4)_2$, $K_3Na(CrO_4)_2$, $K_3Na(SeO_4)_2$, $K_3Na(MoO_4)_2$ and $K_{2.5}Na_{1.5}(MoO_4)_2$; the e.s.d.'s are calculated from the uncertainty of the occupation ('LTP' and 'HTP' are the abbreviations for the low- and high-temperature phases, respectively)*

	$K_3Na(SO_4)_2$,	$K_3Na(CrO_4)_2$ LTP	$K_3Na(CrO_4)_2$ HTP	$K_3Na(SeO_4)_2$ LTP	$K_3Na(SeO_4)_2$ HTP	$K_3Na(MoO_4)_2$ LTP	$K_{2.5}Na_{1.5}(MoO_4)_2$
K(1)	1.39	1.18	1.16	1.18	1.12	1.07	1.02 (1)
K(2)	1.00	0.96	0.91	0.91	0.82	0.93	0.97 (1)
Na	1.24	1.33	1.32	1.26	1.20	1.17	1.25

The structures of $K_3Na(MoO_4)_2$ and $K_{2.5}Na_{1.5}(MoO_4)_2$ closely resemble $K_3Na(SeO_4)_2$, $K_3Na(CrO_4)_2$ and $K_3Na(SO_4)_2$. Nevertheless, the environment of both potassiums in either $K_3Na(MoO_4)_2$ or $K_{2.5}Na_{1.5}(MoO_4)_2$ (Table 6) slightly differs from that in the sulfate, chromate and selenate. There are nine oxygens around the K(1) cation in the molybdates in contrast to ten oxygens in the other members of the family. These nine oxygens from the molybdates are distributed into two shells composed of one and eight oxygens, while in the latter compounds there are clearly differentiated coordination spheres composed of 1 + 6 + 3 oxygens. In all these compounds there is one oxygen with a particularly short bond, K(1)—O(1) $\simeq$ 2.55 Å.

This short K(1)/Na(1)—O bond (2.55 Å) is most probably the reason why excess Na enters the position of K(1). This bond length equals, in fact, the sum of the crystal radii of Na coordinated by nine oxygens (rNa^+ = 1.38 Å) and O (rO^{2-} = 1.24 Å; Shannon, 1976).

There are 8 + 2 oxygens around K(2) in the molybdates; this also differs from the 6 + 6 coordination of K(2) in $K_3Na(SeO_4)_2$, $K_3Na(CrO_4)_2$ and $K_3Na(SO_4)_2$.

The distribution of the longer and shorter bonding distances within the molybdate anion in the stoichiometric compound is similar to those in the selenate and chromate. The shorter Mo—O(1) distance in the stoichiometric compound indicates librational movement (Table 6). In the non-stoichiometric compound the distribution of the bonding distances within the anion is somewhat different compared with the other compounds.

Therefore, the physical meaning of the Mo—O bond-length correction is dubious in $K_{2.5}Na_{1.5}(MoO_4)_2$ and it is given in Table 6 just for comparison.

The larger atomic displacement factors and the atomic displacement vectors (Table 7; Abrahams & Keve, 1971), as well as the lower bond-valence sums (Table 8; Brown & Altermatt, 1985), indicate that K(2) is the most loosely bound cation in the molybdates, similarly as in the sulfate, chromate or selenate. However, the dependence of the decreasing values of bond-valence sums for K(2) on the larger size of the anion observed in the sulfate, chromate and selenate does not hold any more for the molybdates. The structures of the molybdates seem to be stabilized by the relative decrease of the bond valences of K(1) and the increase of K(2). This is, of course, a consequence of the rather different environment of the potassiums in the molybdates. It is interesting that the partial substitution by Na causes a slight increase of the bond valences of the K(2) site, but a decrease of K(1). This may be the reason why no phase transition was observed in $K_{2.5}Na_{1.5}(MoO_4)_2$, because the presence of the phase transition in other members of the family seems to be predominantly related to the underbonding of K(2). The difference between the molybdates and other isostructural compounds is also manifested by the values of the atomic displacement vectors which are about twice as large compared with the corresponding ones in $K_3Na(SeO_4)_2$. This may be the reason why no reversible ferroelastic switching is observed. It is, however, possible that at higher temperatures, but still below the phase transition point, the reversible ferroelastic switching under uniaxial stress may develop. However, on the other hand, it should be emphasized that the observation of the domains was hindered by the semitransparency of the crystals.

From the sixfold twinning observed in $K_3Na(MoO_4)_2$ it may be inferred that it tends to solidify from the melt already as the twofold merohedral twin, otherwise, only a threefold twinning pattern in the low-temperature phase would be observed. No phase transition observed in $K_{2.5}Na_{1.5}(MoO_4)_2$ implies that this compound solidifies as a sixfold twin, a combination of merohedral and pseudo-merohedral twinning. The DSC experiment indicates that non-stoichiometry of a given ratio of K/Na causes the monoclinic distortion to be present after the compound solidifies from the melt. However, seemingly the germs of stoichiometric and non-stoichiometric compounds tend to form with the same type of twinning (twofold twinning) from the melt. It is worthwhile pointing out that in the minor part of crystals of $K_3Na(CrO_4)_2$ grown from aqueous solution at room temperature, *i.e.* above the phase transition, twofold merohedric twins were observed (Fábry, Breczewski & Madariaga, 1994).

The analogous phase transition as well as the monoclinic distortion seem to be very probable in $K_3Na(WO_4)_2$.

Mrs E. Kamarádová and Dr Z. Jirák from the Institute of Physics of the Czech Academy of Science are thanked for their help with the preparation of the samples. The support of this study by grants 203/96/0111 and 202/96/0085 of the Grant Agency of the Czech Republic is gratefully acknowledged.

References

Abrahams, S. C. & Keve, E. T. (1971). *Ferroelectrics*, **2**, 129–154.

Becker, P. J. & Coppens, P. (1974). *Acta Cryst.* A**30**, 129–147.

Bergerhoff, G., Hundt, R., Sievers, R. & Brown, I. D. (1983). *J. Chem. Inf. Comput. Sci.* **23**, 66–69.

CRYSTIN (1995). Crystal Structure Information System. Inorganic Crystal Structure Database, D-76344 Eggenstein–Leopoldshafen, Germany.

Brown, I. D. & Altermatt, D. (1985). *Acta Cryst.* B**41**, 192–197.

Burnett, M. N. & Johnson, C. K. (1996). *ORTEP*III. *Oak Ridge Thermal Ellipsoid Plot for Crystal Structure Illustrations*. Report ORNL-6895. Oak Ridge National Laboratory, Tennessee, USA.

Dušek, M. (1993). *PICTUR. Program for Molecular Graphics*. Institute of Physics, Czech Academy of Science.

Enraf–Nonius (1989). *CAD-4 Software*. Enraf–Nonius, Delft, The Netherlands.

Fábry, J. (1993). *ZPRAC. Program for Data Reduction*. Institute of Physics, Czech Academy of Science.

Fábry, J., Breczewski, T. & Madariaga, G. (1994). *Acta Cryst.* B**50**, 13–22.

Fábry, J., Breczewski, T. & Petříček, V. (1993). *Acta Cryst.* B**49**, 826–832.

Hall, S. R. (1981). *Acta Cryst.* A**37**, 517–525.

Krajewski, T (1990). Personal communication.

Krajewski, T., Mroz, B., Piskunowicz, P. & Breczewski, T. (1990). *Ferroelectrics*, **106**, 225–230.

Krajewski, T., Piskunowicz, P. & Mroz, B. (1993). *Phys. Status Solidi A*, **135**, 557–564.

Madariaga, G. & Breczewski, T. (1990). *Acta Cryst.* C**46**, 2019–2021.

Mehrotra, B. N., Eysel, W. & Hahn, Th. (1977). *Acta Cryst.* B**33**, 305–306.

Mroz, B., Kiefte, H., Clouter, M. J. & Tuszynski, J. A. (1992). *Phys. Rev. B*, **43**, 641–648.

Nardelli, M. (1995). *J. Appl. Cryst.* **28**, 659.

Okada, K. & Ossaka, J. (1980). *Acta Cryst.* B**36**, 919–921.

Petříček, V. (1995). *The SDS System. Program Package for X-ray Structure Determination*. Institute of Physics, Czech Academy of Science.

Shannon, R. D. (1976). *Acta Cryst.* A**32**, 751–767.

Templeton, D. H. & Templeton, L. K. (1978). *AGNOSTIC. Program for Absorption Correction*. University of California, Berkeley, CA, USA.

The Powder Diffraction File (1996). *PDF*-2. Sets 1–45. International Centre for Diffraction Data, USA.